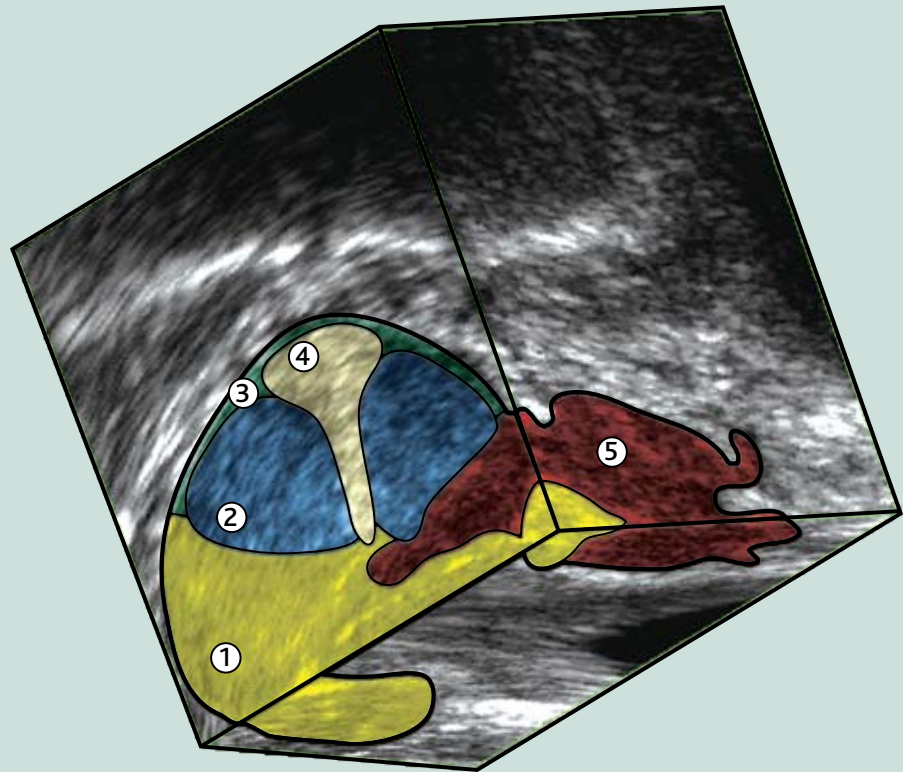


3D Ultrasonography of the Prostate

 Application Note



Transverse and Coronal P-A view together with left longitudinal projection

1. Peripheral zone
2. Transition zone
3. Anterior Fibromuscular Stroma
4. Verumontanum
5. Lesion (sin.) extending through the periprostatic capsule

3D Ultrasonography of the Prostate

Bjørn Fortling, Market Manager, B-K Medical

Accurate staging is crucial for determining the treatment of prostate cancer. Any technique that could overcome the spatial limitations of traditional 2D ultrasound imaging could result in improved staging of disease. In studies of the prostate, 3D ultrasonography has improved staging accuracy compared to 2D ultrasonography (1).

Ultrasound as a diagnostic tool for prostate lesions

Prostate cancer is a major public health issue. In both the United States and Europe, it is the second greatest cause of cancer deaths among men (2,3). Accurate staging is critical to the management of prostate cancer and is particularly significant when selecting candidates for either a radical prostatectomy or low-dose rate (LDR) prostate brachytherapy. If an extracapsular tumor extension goes undetected, the risk that treatment will fail may increase (4,5).

Current methods for local staging include:

- digital rectal examination
- content of PSA (prostate-specific antigen) in serum
- conventional transrectal ultrasound
- endorectal magnetic resonance imaging

All of these methods lack sensitivity, and understaging of up to 50% of cancers has been reported (4-12).

By far the most common method of detecting tumors is transrectal prostate ultrasound combined with random multiple biopsies – often sextant, sometimes even more.

Standard biopsies take samples of specimens from the prostate gland's peripheral zone, an area that extends from the periprostatic capsule to the boundary of the transition zone, with a distance of about 15 mm (see Figures 1 and 2 and "Anatomy

of the Prostate Gland," on next page). The chances of detecting smaller tumors can be improved by increasing the number of biopsy cores taken and by repeating the biopsies, but there is no evidence that the accuracy of staging is also increased (13,14,15).

Recent studies report only 50% to 70% accuracy, due to various factors, including assessment of the spatial relationship between focal lesions and the relatively invisible prostate capsule (8,9,12). Infiltrating prostate cancer that is evenly spread throughout the tissue may not be visible to conventional 2D ultrasound. Furthermore, cancers that are a combination of nodules and infiltrating disease may appear much smaller than their actual size (Fig. 3).

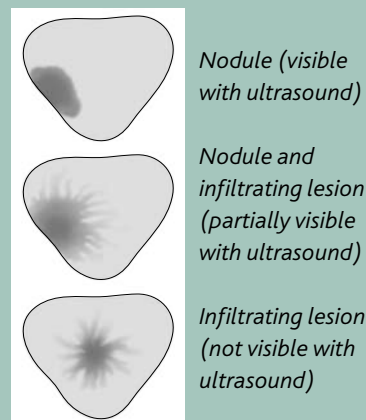


Fig. 3. The ability of ultrasound to detect prostate cancer depends partly on the type of lesion present.

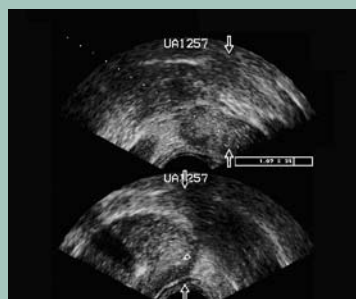


Fig. 1. Transducer rotated for biopsy of the prostate's peripheral zone from the periprostatic capsule to the transition zone boundary.

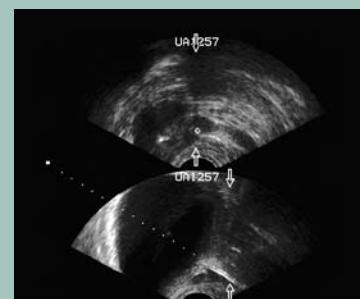


Fig. 2. Biopsy of the 'beak' area, targeting the peripheral zone and the central zone where the central zone interfaces with the seminal vesicles.

Imaged with B-K Medical's type 8808 simultaneous biplane transducer.

Anatomy of the prostate gland

For ultrasound purposes, the prostate can be said to consist of five zones: three glandular (the peripheral zone, transition zone and central zone) and two non-glandular (the periurethral zone and the fibromuscular stroma). The semi-transparent schematic drawings (Figures 4, 5 and 6) represent the ultrasound anatomy of the prostate.

The peripheral zone

The peripheral zone makes up 70% of the glandular tissue. Eighty to 85% of prostate cancers arise here (16).

A healthy peripheral zone displays a homogeneous isoechoic ultrasound pattern.

The "surgical capsule" that separates the peripheral zone from the transition zone appears as a distinct boundary in ultrasound.

The transition zone

The transition zone consists of two separate lobes that lie superior to the verumontanum, lateral to the proximal urethra, and posterior to the fibromuscular stroma.

The transition zone is the site of benign prostatic hyperplasia (BPH). In a non-hypertrophied prostate gland, it makes up 5% of the glandular tissue. Enlargement of the transition zone due to BPH may alter the contour of the prostate in older men, compressing the peripheral zone or displacing it laterally.

Ten to 20% of prostate carcinomas arise in the transition zone.

The central zone

The central zone makes up 25% of the glandular tissue. Five to 10% of carcinomas arise here.

The central zone lies posterior to the urethra and superior to the verumontanum and surrounds the ejaculatory ducts.

The anterior fibromuscular stroma

The anterior fibromuscular stroma forms the anterior surface of the gland. It may be up to 1 cm thick, but thins out over the distal portion of the gland. The anterior fibromuscular stroma is more prominent

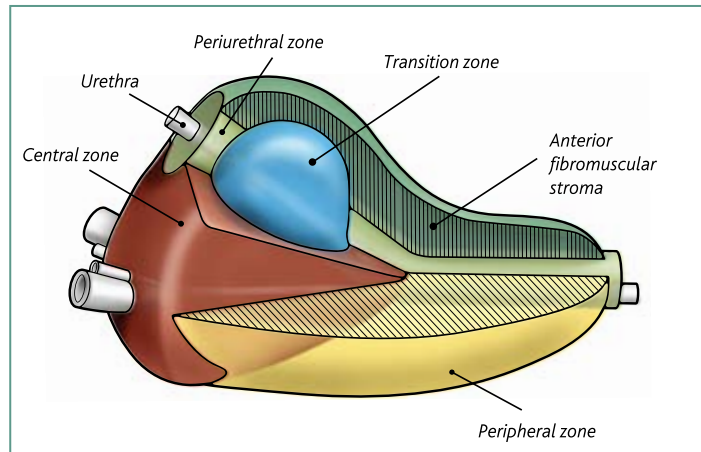


Fig. 4. Ultrasound anatomy of the prostate – sectional view.

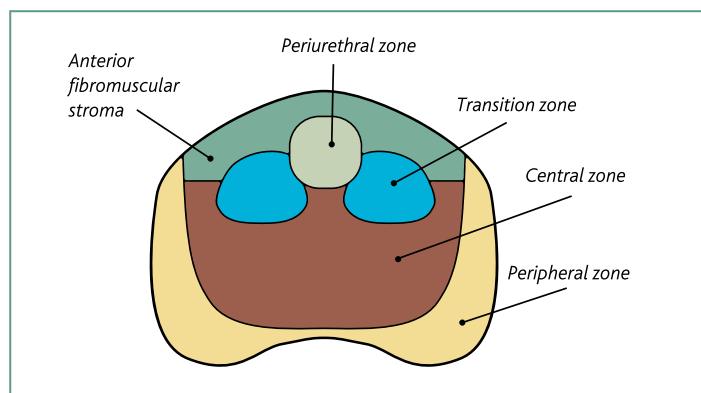


Fig. 5. Ultrasound anatomy of the prostate – transverse section.

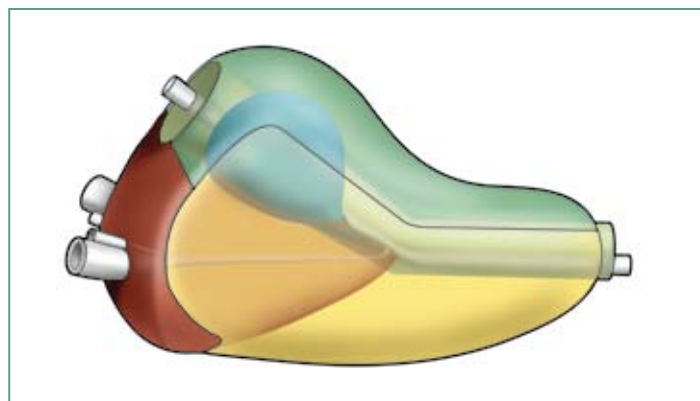


Fig. 6. Ultrasound anatomy of the prostate – semitransparent view.

sonographically in younger, non-BPH patients. It is thought that it may be a barrier to the spread of cancer.

The periurethral zone

The periurethral zone is a mid-line structure of cylindrical, internal smooth muscle sphincter that runs from the base of the verumontanum to the back of the bladder neck. Its function may be to prevent semen

from flowing backwards into the bladder.

The periurethral zone includes the internal urethral sphincter, while the external sphincter is distal to the apex of the prostate.

Advantages of 3D ultrasonography

A key limitation of 2D ultrasound imaging is the considerable lack of in-depth information due to the requirements of keeping the lateral resolution as high as possible.

3D gives access to a new, wider range of viewing planes that are unavailable with 2D scanning (Figure 7).

3D ultrasonography reconstructs a "volume" from 2D scans. This volume can be analyzed using multiplanar viewing, making it possible to see, for example, the coronal view of the prostate. 3D ultrasonography permits quantitative examinations and provides excellent measurement capabilities.

Furthermore, acquired 3D data sets enable completely new post-processing techniques where, for example, the data block can be made semi-transparent, which reveals additional in-depth information.

A major advantage of working with the 3D system is that images used for diagnosis are totally reproducible. Using the original electronic data, images can be reviewed as many times as needed. 3D imaging can give more flexibility to doctors because they can diagnose offline when it is most convenient for them and the patient. This can also contribute to faster patient turnaround.

The specific benefits of 3D ultrasonography of the prostate

3D ultrasonography enables a simultaneous view of the sagittal, transverse and, of especial importance, the posterior-anterior coronal view of the gland to detect possible extra-capsular tumor extension. With such a view of the prostate, doctors get an invaluable tool for diagnostics with 3D imaging. They can more easily distinguish the zones of the prostate and see small lesions.

3D prostate imaging makes spatial relationships much clearer, so urologists can better assess the extent of disease. It provides valuable information that can be used when selecting patients for alternative therapies, for example external beam radiation or prostatectomy/radioactive seed implantation. In particular, it may be easier to determine whether the "prostatic capsule" has been penetrated, a key factor in tumor staging. The 3D data set is acquired in a precise, controlled manner, and can be evaluated at any depth, plane or angle. It can easily be saved for interpretation offline.

3D ultrasonography vs. MRI

The other imaging modality of current interest is endorectal MRI, which has been reported to have a staging accuracy ranging from 60 to 80%. However, endorectal MRI is more expensive than transrectal ultrasonography, is not universally available and needs special expertise to interpret the images. In contrast, 3D image reconstruction can be easily incorporated into conventional transrectal ultrasonography, and is less expensive and easily interpreted by experts in conventional ultrasonography.

Overall, 3D ultrasonography helps urologists perform more thorough volume studies, reduce exam time and increase patient comfort. The following section looks at a specific study that shows how 3D ultrasonography can improve diagnosis of prostate cancer.

A 22% increase in overall staging accuracy

A study (1) in the *Journal of Urology*, Vol. 162, 18-1321, October, 1999, determined the value of 3D reconstruction of conventional transrectal ultrasonography images of clinically localized prostate cancer in patients undergoing radical prostatectomy. A total of 36 patients with a median age of 63 years (range 54 to 70) were studied. All patients underwent conventional 2D transrectal ultrasonography with prostatic biopsy and tumors were staged using the 1997 TNM

classification. Additional ultrasound-guided biopsies of any hypoechoic lesions were also performed. Between three and six weeks later, transrectal ultrasonography was performed in all cases to acquire images that were then reconstructed into 3D volumes immediately prior to surgery.

The sequence of acquired images was reconstructed to make a 3D data set which was viewed interactively using the same computer and software. The software allows the 3D image to be sliced in any plane and any orientation, and rotated in any direction. The display software allows up to three surfaces of the prostate to be viewed simultaneously in a 3D rendering. The accuracy, sensitivity, specificity and positive and negative predictive values were calculated for detecting extracapsular disease using 3D imaging.

Pathological analysis revealed cancer in 63 of 72 slides of prostate (bilateral in 25 patients) and 15 sites of tumor infiltration beyond the prostatic capsule in 10 patients.

Sensitivity and specificity for laterality for cancer detection were 63% and 66%, respectively, for 3D imaging, which was no different from that obtained using 2D transrectal ultrasonography. The 3D imaging predicted 12 of the 15 sites of tumor infiltration beyond the prostatic capsule in 9 of 10 patients. Of the sites not detected, two were posterolateral and one was anterior. There was one false-positive prediction of extracapsular tumor.

For detection of extracapsular tumor, sensitivity was 80%, specificity 96%, positive predictive value 90% and negative predictive value 96%. 3D ultrasound accurately staged 1 of 2 cases with seminal vesicle involvement. Overall staging accuracy of 3-D imaging was 94%. Conventional transrectal ultrasonography was accurate in 72% of cases.

Overall, 3D reconstruction of 2-D transrectal ultrasonography images resulted in a 22% increase in overall staging accuracy which was statistically significant (italics added).

Visualization of the lesion in 3 planes appeared to allow improved assessment of capsular disruption. With the additional coronal view of the prostate—instead of a single transverse scan slice of the prostate seen on 2D transrectal ultrasonography—the 3D images provide an added surface to be visualized. This surface could be the lateral, posterior, anterior, superior or inferior surface of the prostate, or a through section of the gland, where the posterior surface of the prostate shows tumor infiltration beyond the periprostatic fat.

Today, the 3D acquisition is performed using a precision motorized device, and a much higher number of transaxial images are interpreted for the total image reconstruction (typically several hundred). This technique has resulted in a much improved spatial resolution.

Volume Render Mode

The acquisition of a 3D data set and the underlying techniques are different from application to application.

One common technique, Surface render mode, is used, for example, to capture images of an unborn baby's facial contours.

Surface rendering techniques only give good results when a surface is available to render. This explains why the most common example is that of a fetus imaged while floating in amniotic fluid. These techniques fail when a strong surface (a shift in the ultrasound impedance of tissue) cannot be found, such as in the subtly layered structures within the anal canal, rectal wall, prostate etc.

High resolution 3D ultrasound acquires four to five transaxial images per 1mm of acquisition length (in the Z-plane). Due to this resolution in the Z-plane, which typically is close or equal to the axial- and transverse resolution of the 2D image, 3D post processing facilities can offer significantly more features than available in relatively low resolution 3D data sets.

An ultrasound image has under normal circumstances no depth due to the requirements of keeping lateral resolution of the image as high as possible. The image may be compared to looking at a photographic

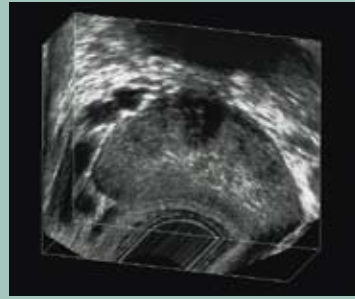


Fig. 7. 24Y Male right peripheral zone, (volume rendered) 3D image. Note the normal size of the peripheral zone which most probably occupies around 70% of the glandular tissue volume.

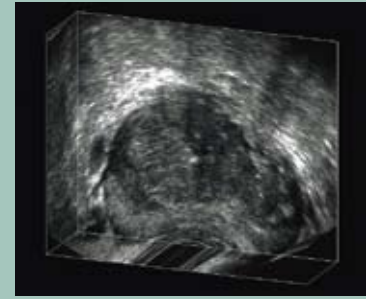


Fig. 8. 61Y Male right peripheral zone, (volume rendered) 3D image. Note the peripheral zone is compressed by the large adenoma in the right side, resulting in a narrow band only in the oral/caudal direction.

image on a piece of paper. Ray tracing techniques may overcome this limitation.

Volume rendering mode techniques (see Figures 7 and 8) use a ray tracing model as their basic operation. A ray or beam is projected from each point on the display screen back into and through the volume data. As the ray passes through the volume data it reaches the different elements (voxels) in the data set. Depending on the various render mode settings, the data from each voxel may be discarded, it may be used to modify the existing value of the ray, or it may be stored for reference to the next voxel and used in a filtering calculation. All of these calculations result in the current color or intensity of the ray being modified in some way. At some point, the ray reaches a limit to its ability to penetrate the volume data. The current color or intensity value that the ray has acquired at this point is then shown on the display screen at the position where the ray trace started.

Some rendering modes also apply global operations to the ray calculations: Maximum Intensity Projection (MIP) tries to find the brightest or most significant color or intensity along a ray path.

Transparent modes allow the separation of color and intensity data and selective control of the transparency of the two components. Using this method, it is possi-

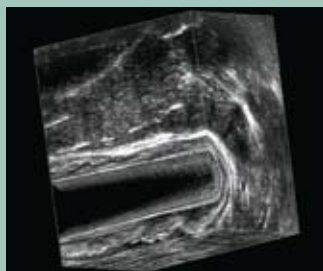
ble to reduce the intensity of the gray scale voxels so that they appear as a light fog over the color information. Color information hidden behind an obstruction can then be made visible. Both of these methods require the ray trace to pass through the entire volume and, in the case of transparent display methods, to pass through the entire volume twice.

The Volume render effect may in particular be dramatic if a number of voxels inside an acquired 3D data set are produced from scanning hypoechoic structures. A hypoechoic focal lesion in the prostate is a good example. Voxel values behind, for example, a strongly reflective interface will also result in an illusion of looking into a semi-transparent dark cavity in the anatomy.

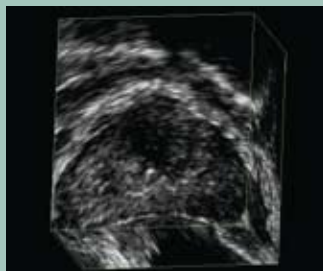
Comparison of 2D and 3D ultrasound images of the prostate

2D

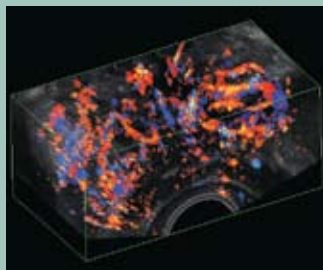
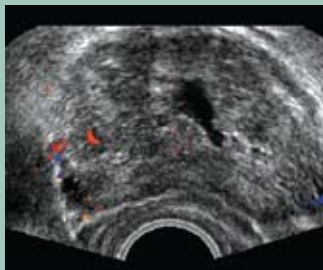
3D



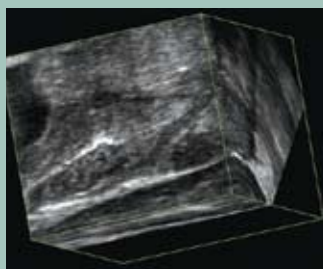
52Y patient post-LDR seed implantation



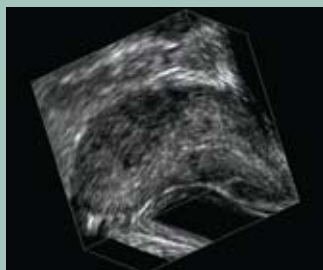
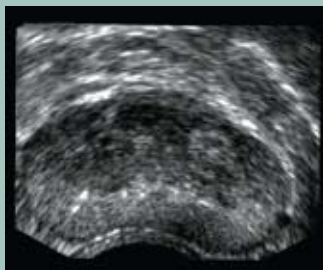
64Y Patient with prostate tumor; peripheral zone inferior lateral (sin.)



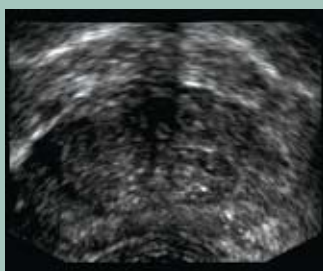
68Y Patient CFM plus TURP cavity



69Y Patient with small prostate tumor seen on sagittal plane



72Y patient with prostate tumor; peripheral zone inferior lateral (sin.)



79Y patient with BPH and catheter

Some examples of urology transducers from B-K Medical with 3D imaging capabilities

3D ultrasonography from B-K Medical is available on a wide range of our scanners as a standard option, and many of our urology transducers offer 3D imaging capabilities.



8848



8818



8808



8658



8667

1) Sudhanshu Garg, Bjørn Fortling, David Chadwick, Mary C. Robinson and Freddie C. Hamdy:

Staging of prostate cancer using 3Dimensional transrectal ultrasound images: a pilot study

J. Urol. 1999; Vol. 162: 18-1321

2) Mettlin C, Jones G, Averett H, Gusberg S and Murphy G:

Defining and updating the American Cancer Society guidelines for cancer-related checkup: Prostate and endometrial cancers. *Cancer* 1993; 42:42

3) Rietbergen J B W, Kranse R, Kirkels W J, Koning H J D and Schroder F H:

Evaluation of prostate-specific antigen, digital rectal examination and transrectal ultrasonography in population-based screening for prostate cancer: Improving the efficiency of early detection.

Brit. J. Urol. 1997; 79:57

4) Epstein J I, Carmichael M J, Pizov G and Walsh P C:

Influence of capsular penetration on progression following radical prostatectomy: A study of 196 cases with long-term follow up.

J. Urol. 1993; 150:135

5) Epstein J I:

Incidence and significance of positive margins in radical prostatectomy specimens.

Urol. Clin. N. Amer. 1996; 23: 652

6) Huch B R, Boner J A, Debatin J F, Trinkler F, Knonagel H, Von H A, Helfstein U, and Krestin G P:

Optimization of prostate carcinoma staging: Comparison of imaging and clinical methods.

Clin. Rad. 1995; 50:593

7) Perrotti M, Kaufman R J, Jennings T A, Thaler H T, Soloway S M, Rifkin M D and Fisher H A:

Endo-rectal coil magnetic resonance imaging in clinically localized prostate cancer: Is it accurate?

J. Urol. 1996; 156:106

8) Presti J J, Hricak N, Narayan P A, Shinohara K, White S and Caroll P R:

Local staging of prostatic carcinoma: Comparison of transrectal sonography and endorectal MR imaging.

AJR 1996; 166:103

9) Rifkin M D, Zerhouni E A, Gatsonis C A, Quint L E, Paushter D M, Epstein J I, Hamper U, Walsh P C and McNeil B J:

Comparison of magnetic resonance imaging and ultrasonography in staging early prostate cancer. Results of a multi-institutional cooperative trial.

New Engl. J. Med. 1990; 323:621

10) Salo J O, Kivisaari L, Rannikko S and Lehtonen T:

Computerized tomography and transrectal ultrasound in the assessment of local extension of prostatic cancer before radical retropubic prostatectomy.

J. Urol. 1987; 137:435

11) Scardion P T, Shinohara K, Wheeler T M and Carter S S:

Staging of prostate cancer: Value of ultrasonography.

Urol. Clin. N. Amer. 1989; 16:713

12) Smith J A Jr., Scardion P T, Resnick M I, Hernandez A D, Rose S C and Egger M J:

Transrectal ultrasound versus digital rectal examination for staging of carcinoma of the prostate: Results of a prospective, multi-institutional trial.

J. Urol. 1997; 157:902

13) Norberg M, Egevad L, Holmberg L, Sparen P, Norlen B J and Bush C:

The sextant protocol for ultrasound-guided transrectal core biopsies of the prostate.

J. Urol. 1997; 50(4):562

14) Hodge K K, McNeal J E, Terris M K and Stamey T A:

Random systematic versus directed ultrasound-guided transrectal core biopsies of the prostate.

J. Urol. 1989; 142(1):71

15) Epstein J I, Walsh P C, Sauvagot J and Carter H B:

Use of repeat sextant and transition zone biopsies for assessing extent of prostate cancer.

J. Urol. 1997; 158:1886

16) Stamey T A:

Making the most out of six systematic sextant biopsies.

Urology 1995; 158:1886

World Headquarters
Mileparken 34
DK-2730 Herlev
Denmark

Tel: +45 44 52 81 00 • Fax: +45 44 52 81 99 • www.bkmed.com

*With more than 30 years of
commitment to ultrasound
innovation, B-K Medical
specializes in the develop-
ment, manufacture and
distribution of dedicated
ultrasound solutions.
B-K Medical has its head-
quarters in suburban
Copenhagen, Denmark
and has offices and
distributors throughout
the world.*

Sales offices

B-K Medical Systems, Inc.
250 Andover Street
Wilmington, MA 01887
USA
Tel: (1) 978-988-1078
/ 800 876-7226
Fax: (1) 978-988-1478

B-K Medical Benelux NV
Generaal de Wittelaan 19/7
2800 Mechelen
Belgium
Tel: (32) 1528 0600
Fax: (32) 1529 1025

**B-K Medical Medizinische
Systeme GmbH**
Pascalkehre 13
25451 Quickborn
Germany
Tel: (49) 4106 99 55-0
Fax: (49) 4106 99 55-99

B-K Medicale S.r.l.
Via Tulipani, 3/B
20090 Pieve Emanuele MI
Italy
Tel: (39) 02 90 78 13 47
Fax: (39) 02 90 78 19 05

B-K Medical Norge
Nesru Senter, Fekjan 7B
1394 Nesbru
Norway
Tel: (47) 66 77 45 77
Fax: (47) 66 77 45 78

B-K Medical AB
Månskärsvägen 9
141 75 KUNGENS KURVA
Sweden
Tel: (46) 8-744 02 11
Fax: (46) 8-744 02 12

B-K Medical (Asia) Pte. Ltd.
6 Temasek Boulevard #27-06
Suntec City Tower Four
Singapore 038986
Singapore
Tel: (65) 6887 5270
Fax: (65) 6887 5272

B-K Medical (UK)
11 Grove Park
Waltham Road, White
Waltham
Berkshire SL6 3LW
United Kingdom
Tel: (44) 1628 825-770
Fax: (44) 1628 826-970

Represented in

Argentina	Kuwait
Australia	Latvia
Austria	Lebanon
Bangladesh	Lithuania
Belgium	Luxembourg
Bolivia	Malaysia
Brazil	Malta
Bulgaria	Mauritius
Canada	The Netherlands
Chile	New Zealand
P. R. of China	Norway
Colombia	Pakistan
Costa Rica	Peru
Croatia	Philippines
Czech Republic	Poland
Denmark	Portugal
Ecuador	Romania
Egypt	Russia
Estonia	Saudi Arabia
Finland	Serbia and Montenegro
France	Singapore
Germany	Slovak Republic
Ghana	Slovenia
Greece	South Africa
Guatemala	Spain
Hong Kong	Sweden
Hungary	Switzerland
Iceland	Syria
India	Taiwan
Indonesia	Thailand
Iran	Tunisia
Iraq	Turkey
Ireland	UAE
Israel	UK
Italy	Ukraine
Japan	Uruguay
Jordan	USA
Kazakhstan	Venezuela
Korea	Vietnam

Please contact World Headquarters for further information